Materials Today: Proceedings xxx (xxxx) xxx

Contents lists available at ScienceDirect

Materials Today: Proceedings

journal homepage: www.elsevier.com/locate/matpr

Towards the ultrafast optical nanopore platform for single molecule sensing

Seong Soo Choi [a,*], Sae-Joong Oh [a], Yong Min Lee [a], Hyun Tae Kim [b], Soo Bong Choi [b], Byung Seong Bae [c]

[a] Research Center for NanoBio Science, SunMoon Unviersity, Ahsan, Chungnam 31460, South Korea
[b] Department of Physics, Incheon National University, Incheon 22010, South Korea
[c] School of Electronics and Display Engineering, Hoseo University, Ahsan, Chungnam 31499, South Korea

ARTICLE INFO

Article history:
Received 29 November 2019
Accepted 17 January 2020
Available online xxxx

Keywords:
Nanopore platform
Nanoscale double slits
Surface plasmon
Au, Focused ion beam
Optical biosensor

ABSTRACT

Recently there have been significant interests about fabrication of optical nanopore with its diameter range of 5 nm–10 nm for single molecule analysis and manipulation. However, due to very small amount of the optical intensity through the tiny size of the nano-aperture much smaller than the optical wavelength, the optical intensity enhancement via plasmonic effect by using pore array or periodic groove patterns have been tried. Also, the double slits with nanoscale width are reported to provide the constructive periodic modulation for the transverse-magnetic (TM) wave mode. In this report, the Au aperture arrays sidelined with the nanoscale double slit, and surrounded by 4 nanoscale slits have been fabricated with optical characterization in the visible range.

Selection and Peer-review under responsibility of the scientific committee of the EurasiaNanotechnology Conference.

1. Introduction

About 60 years ago, the biological cell counter with an electrical detection technique was invented by Dr. Coulter [1]. Due to fast developing nanofabrication technology, the smaller nanobio device for single molecule detection has been tested and manufactured [2]. The fabricated portable nanopore device by using electrical detection technique is reported to have high error rates [2,3], possibly due to the electrical double layer formed in the nanopore channel. Considering the fact that most biosensors are utilizing the optical detection technique, the optical pore device can be an excellent candidate for the next generation single molecule sensor. However, the tiny nano-aperture with its diameter of ~10 nm or less would have negligible optical transmission from Bethe's law; $T \sim (d/\lambda)^4$. Optical transmission through the tiny nano-aperture should be enhanced either by providing the groove patterns or periodic arrays [4]. The nanopore with ~nm diameter for an optical detection technique has yet to be fabricated.

The enhancement of light transmission through a nano-aperture surrounded by periodic patterns on the input side of a flat plane has been also reported [4], and a directional beaming effect through an aperture with a periodic pattern on the exit side of a flat membrane has been also reported [5]. We previously reported fabrication of the nano-aperture surrounded by the periodic patterns on the outside of the pyramidal probes to improve the low transmittance of light through the nanosize aperture [6–8]. Huge optical intensity enhancement of $\sim 10^3$ fold increase through a pyramidal aperture has been reported for the groove patterns whose pitch matched the surface plasmon wavelength, which can be attributed to the coupling of a backward diffracted surface wave with the patterned grooves on the exit side of the pyramid. Even without a nano-aperture on top of the an elliptically patterned pyramid, a huge 10^3-fold increase is also reported in the transmitted optical power due to the strong coupling of the surface plasmonic modes with the photonic modes of the input beams. The enhancement of light transmission through a nanometer-sized aperture surrounded by the periodic patterns on the input side of a flat plane has been previously reported, and a directional beaming effect through an aperture with a periodic pattern on the exit side of a flat membrane has been also reported [5]. For optical transmission through a real nano-aperture array, the shape of the nanoholes in metals can modulate their optical transmission properties, and a huge increase (10^4 times) in the second harmonic generation from a metal [9], a 40 times increase in the fluorescence of molecules on a metallic surface [10], entanglement preservation through macroscopic plasmon propagation [11]. Strong polarization dependence is observed in the optical transmission through

* Corresponding author.
E-mail address: sscphy2010@gmail.com (S.S. Choi).

https://doi.org/10.1016/j.matpr.2020.01.359
2214-7853/
Selection and Peer-review under responsibility of the scientific committee of the EurasiaNanotechnology Conference.

elliptical nanohole arrays in metals. The degree of polarization is determined by the ellipticity and orientation of the holes; the polarization axis lies perpendicular to the broad edge of the ellipse [12]. The strong polarization dependence of the transmission as a function of the ellipse orientation is similar to the transmission through a subwavelength slits surrounded by the surface corrugation, and to the transmission through metallic nanowire gratings. The polarization of the transmitted light is also found to be strongly dependent on the orientation and geometry of the holes, and the influence of the aspect ratio on the polarization is explained in terms of coupling to the SP modes [12].

We have fabricated the nanopore with its diameter ranging from 10 nm to 3 nm on the on the flat Au thin membrane by using various surface modifications [13–16]. Au-apertures with its diameter ranging from 50 nm to 100 nm were initially drilled by 30 keV Ga focused ion beam technique (FIB), then by using various electron beam irradiations such as field emission electron beam microscopy (FESEM) and transmission electron beam microscopy (TEM), a nanopore with its diameter of 5 nm was formed on the diffused membrane inside the FIB-drilled Au aperture. Optical intensity measurements did not reveal any differences between through the nano-aperture without a diffused Au-C membrane, and through the nano-aperture with a diffused membrane. This can be attributed to the diffused membrane thickness below the Au skin depth ($\ll$20 nm), and low Au atomic concentration ($\ll$50%) on the membrane [12,16].

Classical double slits with micron size slit-width would provide the far field interference patterns, regardless of the polarization states. However, for the nanoscale double slits, the surface plasmonic wave from the nanoscale slits can provide the periodic interference phenomena for the TM wave between the nanoscale slits, which reduces or enhances the intensity of the far-field [17–19]. When the incident light is TM-polarized, electric field aligned perpendicular to the slits, the surface plasmon wave that is excited at one of the slits propagates towards its other slit. For the case of TM polarization, the transmission via slits is seen to be sinusoidally modulated as a function of wave number, and the modulation period becomes inversely proportional to the slit separation. For a TE (transverse electric)-polarized incident beam there will be no modulation. There will be three possible types of physical mechanisms; first, the slits transmit part of the incident radiation, together giving rise to a conventional Young-type interference pattern. Second, each slit scatters part of the incident radiation into a plasmonic channel, bridging the momentum gap between the surface plasmon and free-space radiation. Third, each slit provides a mechanism for back-converting a surface plasmon into free-space radiation. Hence, the strength of each of these sources is enhanced or reduced due to the interference of a photonic and a plasmonic channel. With proper controlling the pitch of the aperture and the nanoscale slits separation gap, the enhanced optical intensity would be obtained. In this report, fabrication and optical characterization in the visible range of the nanopore platform which consists of Au nano-aperture array sidelined with two nano-slits and surrounded by 4 nano-slits will be presented.

2. Experimental procedures

Initially, the ~200 nm Au thin films were deposited on the 5 nm thick SiN commercial TEM grids (www.temwindows.com), followed by dry etching of supporting the SiN membrane. Then, drilling for Au aperture array with its diameter of ~200 nm was followed by using focused Ga ion beam technique (Dual beam Helios, FEI). The nanoscale slits with (~170 nm wide and ~5 μm long) size were also drilled, and electron beam irradiations were carried out by using as transmission electron microscopy (TEM) (JEM-2010, JEM-2100F) and field emission scanning electron microscopy (FESEM, JSM 6400) were utilized. TEM can provide high electron voltages ranging from 100 keV to 300 keV and the currents with ~order of 100 pA, while FESEM (Dual Beam Helios, FEI) will provide the probe current of 1.4nA/nm^2 ranging from 2 keV to 20 keV. Then, its optical characterization was carried out by using a white light using Halogen lamp installed at Nikon TE eclipse microscope with a spectrometer (SpectraPro 2300i (150 g/mm), Princeton Instruments).

3. Experimental results

Fig. 1 presents the large circular aperture with a 15 μm diameter for a calibration of the optical beam (top left), and a single slit with a (~170 nm wide × ~5 μm long) (a). Double slits with double slits with 5 μm separation (b), 10 μm separation (c), 15 μm separation (d), and 20 μm separation are presented (e). Fig. 2 presents TEM images of the 5 μm long slit, and diffused Au particles due to the thermal spike effect during the FIB drilling procedure presented in Fig. 2(b). And the electron beam profile at the electron beam detector through the slit with a ~ 170 nm width is presented in Fig. 2(c).

We investigated the transmitted optical intensities dependent upon the pitches (separations) of the nanoscale slits. Fig. 3 presents the normalized optical peak intensities versus wavelength for the slits with different pitches. The red line (a) and the blue line (b) display the optical intensities for the single slit and for the slits with a 5 μm pitch, respectively. And the green line (c), the violet line (d), and the dark yellow (e) line indicate the normalized peak optical intensities for the slits with 10 μm pitch, 15 μm pitch, and the 20 μm pitch, respectively. The optical intensities for (c), (d) and (e) are weaker than those for the single slit (a), and also for the double slits with a 5 m pitch (b). However, for the 15 μm pitch, the optical intensity in (c) is measured to be greater than those for 10 μm pitch (c). Then, for the 20 μm pitch (e), the optical intensity is measured to be much weaker than those for 10 μm pitch. These optical intensity variations dependent upon the increased slit pitch indicate the constructive interferences for the slits with a 5 μm pitch, and a 15 μm pitch. The periodical interference phenomena dependent upon the pitch is also presented in Table 1. The optical intensity ratio is defined as the total integrated output intensity for the entire optical wavelength divided by the total input intensity (free space intensity). With increasing the separation of the slits from 5 μm to 20 μm, the decreased interference optical intensity is clearly shown. However, the optical ratio (0.1694) from the sample with 15 μm separation is higher than that (0.1004) with 10 μm separation. This could be attributed from periodic modulation effect dependent upon the slit separation.

Fig. 4 presents the (7 × 7) Au aperture arrays on the 200 nm Au deposited film with its pitches of 530 nm in (a), 780 nm in (b), and 1064 nm in (c). The aperture diameters are set to be ~200 nm. And after the optical characterization, the nanoscale double slits were drilled, the width and the length of the drilled nanoscale slit are measured to be ~170 nm wide and ~5 μm long, respectively.

Fig. 5 presents the optical enhancement factor versus input wavelength. The optical enhancement factor is defined as the ratio of the free space input intensity to the output intensity. Highest enhancement factor of 1.72 at 713 nm is presented for (7 × 7) array with a 530 nm pitch, and the enhancement factors of less than 0.5 from the entire wavelength ranging from 550 nm to 800 nm are shown for the (7 × 7) array with 780 nm pitch and 1060 nm pitch in Fig. 5(a). Fig. 6(b) presents the enhancement

Please cite this article as: S. S. Choi, S. J. Oh, Y. M. Lee et al., Towards the ultrafast optical nanopore platform for single molecule sensing, Materials Today: Proceedings, https://doi.org/10.1016/j.matpr.2020.01.359

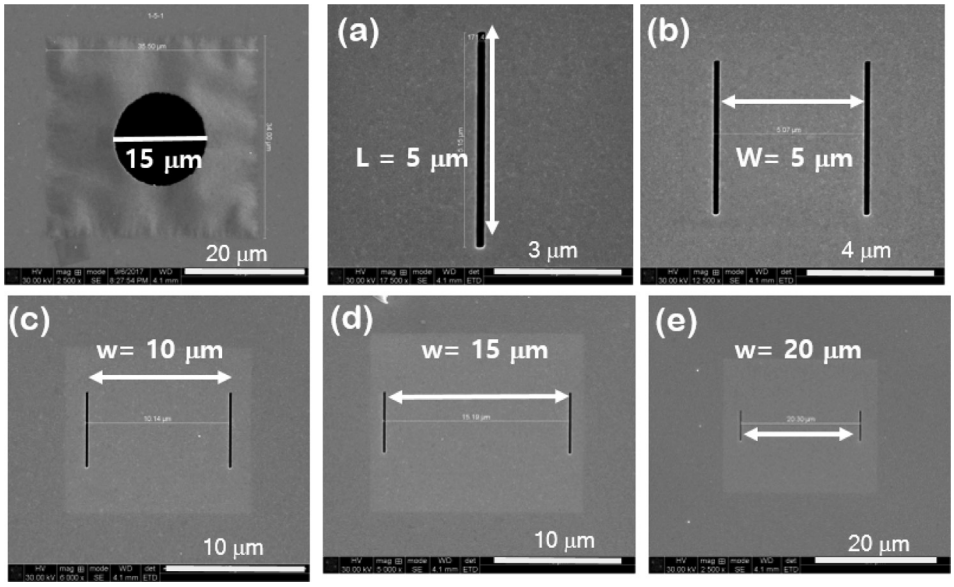

Fig. 1. The FESEM images present a circular hole with a 15 mm diameter as a calibration control sample for the optical characterization (top left), and the 5 μm long single slit (a), double slits with a 5 μm separation (b), a 10 μm separation (c), a 15 μm separation (d), and a 20 μm separation (e).

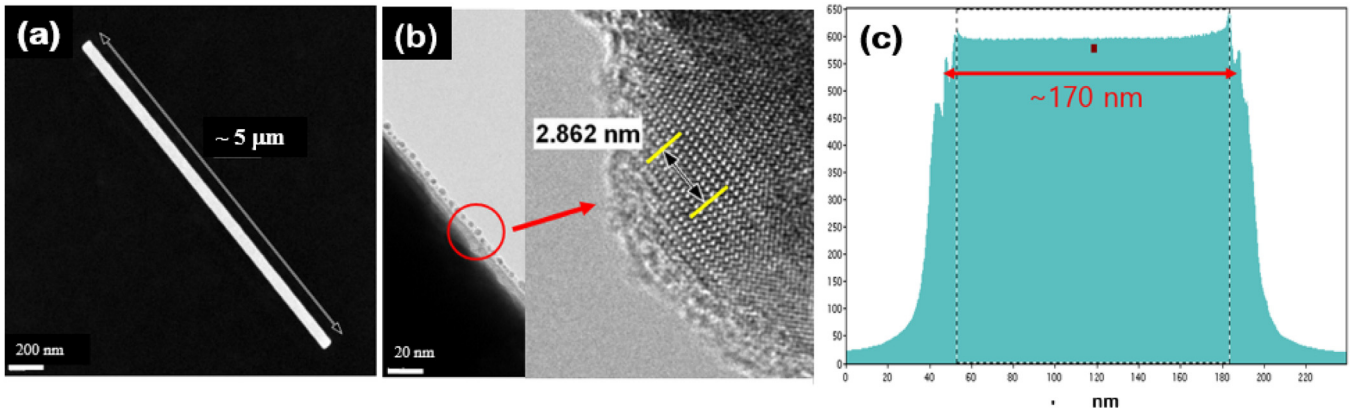

Fig. 2. TEM images show a ~5 μm long single slit (a), the Au nanoparticles formed and diffused on the slit edge due to high temperature effect from the thermal spike during the FIB drilling procedure (b), and an Au nanoparticle with a 2.862 nm width for 10 atomic spacing is presented. An electron beam profile through the ~170 nm wide gap of the slit on the electron beam detector is also shown (c).

factor of 8.36 at 719 peak for the (7 × 7) array with 530 nm pitch, and the enhancement factor less than 2 for the entire wavelength regime ranging from 550 nm to 800 nm. The enhancement increase at the peak from 1.72 to 8.36 can be attributed to the nanoscale slits effect from additional constructive interferences between the surface plasmonic wave arising from the slits and the surface plasmon wave from the (7 × 7) aperture array.

Fig. 6 presents the normalized transmitted optical intensities for the (7 × 7) nano-aperture array with double nano-slits in Fig. 6(a) and surrounded with 4 nano-slits in Fig. 6(b). Huge increase of the transmitted intensity for the sample with double nanoslits can be attributed to the constructive interference phenomena between the periodic wave formed from the double slits and the surface wave from the nano-aperture array. However, the significantly reduced transmitted optical intensity from the aperture array surrounded with the 4 nanoslits could be destructive interference among the surface waves from the nano-aperture array and the surface waves from two double slits.

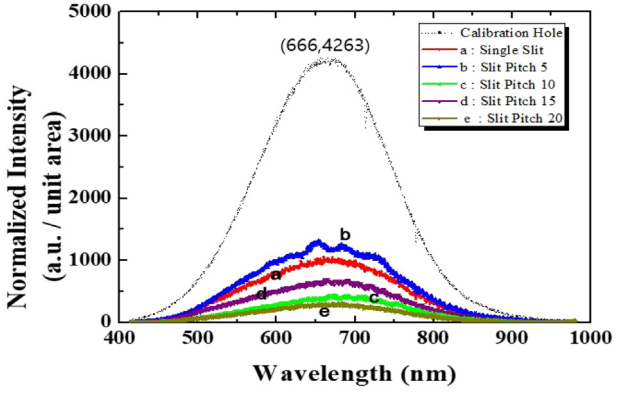

Fig. 3. Presents the normalized optical intensities to slit open gap area through the double nanoscale slits for the pitches versus input wavelength. The dashed line indicates the free space intensity. Red a line and blue b line present the output intensities for single slit, and double slit with a 5 μm pitch. Green c line, violet d line, and dark yellow e line indicate the output intensities from double slits with pitches of 10 μm, 15 μm, and 20 μm, respectively. (For interpretation of the references to colour in this figure legend, the reader is referred to the web version of this article.)

Please cite this article as: S. S. Choi, S. J. Oh, Y. M. Lee et al., Towards the ultrafast optical nanopore platform for single molecule sensing, Materials Today: Proceedings, https://doi.org/10.1016/j.matpr.2020.01.359

Table 1
Please note that the normalized optical intensities for 10 μm pitch, 15 μm pitch and 20 μm pitch are measured to be lower than that of a single slit. In addition, the normalized optical intensity (0.3149) for 5 μm pitch is greater than those for a single slit, and 10 μm pitch, 15 μm pitch and 20 μm pitch. Furthermore, the optical intensities for 5 μm pitch and 10 μm pitch become reduced from 0.3149 to 0.1004, then become increased from 0.1004 to 0.1694. The optical intensities seem to oscillate periodically as the pitches become greater.

Sample name	Pitch	Total area (μm^2)	Integrated intensity	Ratio (I_{out}/I_{free})
21-20-2	Calibration Hole	185.78	886,847.2	1.0000
6-10-1-A	Single Slit	0.87	227,171.8	0.2562
6-10-1-C	5.07 μ m	1.75	279,288.9	0.3149
6-10-1-E	10.14 μ m	1.75	88,999.0	0.1004
6-10-1-G	15.19 μ m	1.75	150,213.9	0.1694
6-10-1-I	20.30 μ m	1.75	62,952.3	0.0710

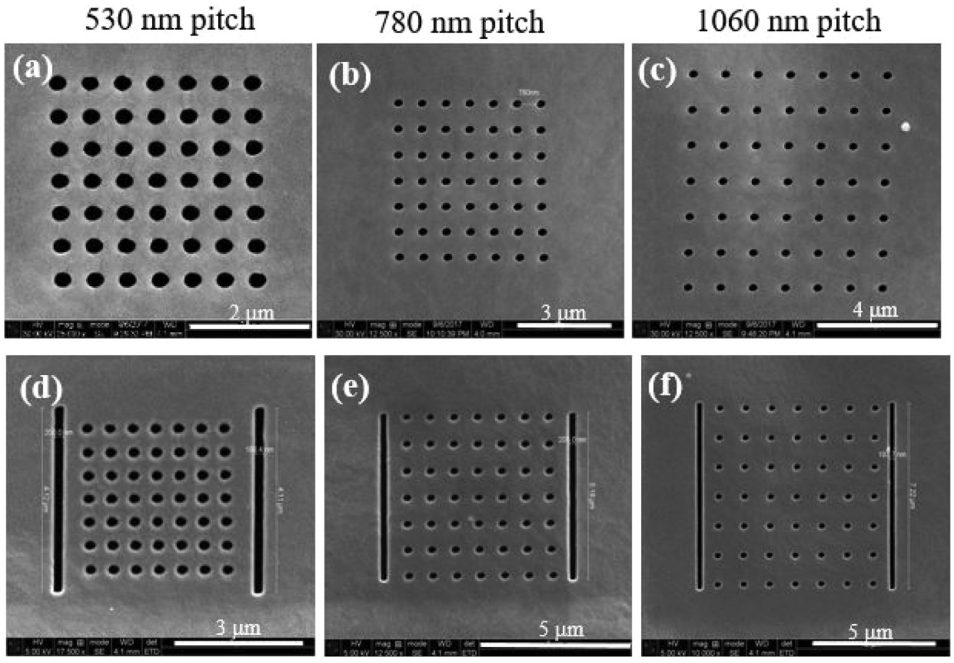

Fig. 4. FESEM images present (7 × 7) arrays with its diameter of ~200 nm, and also circular aperture arrays with pitches of 530 nm, 780 nm, and 1060 nm without nanoscale double slits (a–c), and with double slits (d-f).

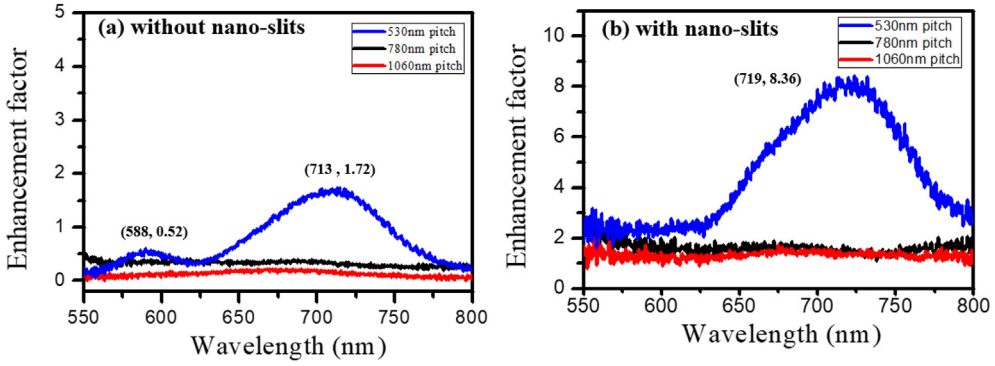

Fig. 5. The Enhancement factors versus input optical wavelength are presented for the (7 × 7) Au nano-aperture array without nanoscale double slit (left, a), and for (7 × 7) array with the slits (right, b). Highest enhancement factor of 1.72 at 713 is presented for (7 × 7) array without double slits for the 530 nm pitch, and the enhancement factor of 8.36 at 719 peak for the (7 × 7) array with double slits for the 530 nm pitch.

4. Discussion

We have fabricated the nanopore platform with nano-aperture array and nanoscale double slits dependent upon the pitch between two slits. For nanoscale double slits without a nano-aperture array, at 5 μm pitch and 15 μm pitch, the optical intensities are measured to be greater than that for a single slit, due to the constructive interference of the surface plasmon wave from the slits. At 10 μm pitch and 20 μm pitch, the optical intensities are found to be weaker than that even for the single slit due to destructive interference from the slits. These observations are agreeable with previous experiments by others.

Please cite this article as: S. S. Choi, S. J. Oh, Y. M. Lee et al., Towards the ultrafast optical nanopore platform for single molecule sensing, Materials Today: Proceedings, https://doi.org/10.1016/j.matpr.2020.01.359

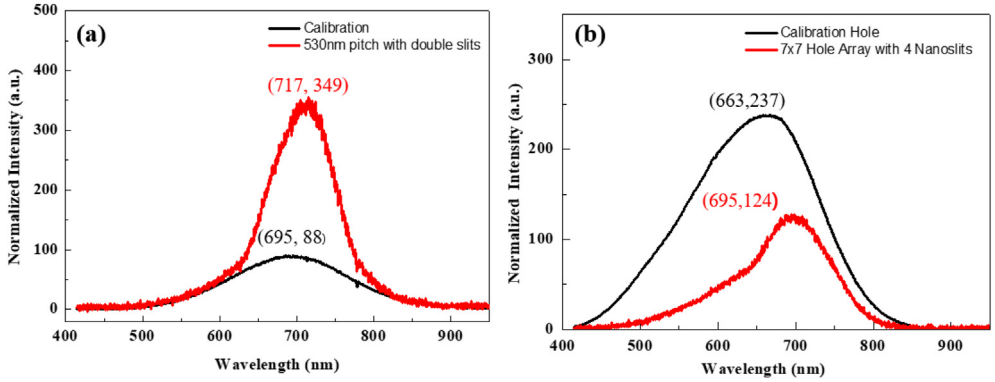

Fig. 6. Presents the normalized intensities for (7 × 7) nano-aperture array with double nanoslits (a), and the aperture array surrounded with 4 nanoslits (b). Huge increase of the transmitted intensity (red line) for the aperture array with the double slits can be attributed to the constructive coupling of the periodic wave between the nanoscale double slits with the transmitted wave from the nano-aperture array. However, the transmitted optical intensity with the significant reduction for the aperture array with 4 nanoscale slits (red line) is presented possible due to the destructive interferences from the transmitted waves and the surface waves. (For interpretation of the references to colour in this figure legend, the reader is referred to the web version of this article.)

For the (7 × 7) nano-aperture array without nanoscale double slits, the highest optical enhancement factor of 1.73 at the 713 nm peak position is presented for the (7 × 7) array with a 530 nm aperture-pitch, among the nano-aperture array with aperture-pitches of 530 nm, 780 nm, and 1060 nm. For the aperture array sidelined with nanoscale double slits, the enhancement factor of 8.36 at 719 peak for the (7 × 7) array with a 530 nm aperture-pitch is observed. The huge enhancement factor increase at the peak position from 1.72 to 8.36 can be attributed to the constructive interferences from the nanoscale double slits, in addition to the surface plasmon resonances among the nano-aperture array.

For the (7 × 7) nano-aperture array surrounded with 4 nanoslits, significant reduction of the optical intensity much weaker than the normalized input intensity is presented. This could be attributed from the destructive interference phenomena from the interaction among the surface waves and the transmitted waves from the nano-aperture array. The detailed physical mechanism for this experimental observation is still under investigation.

5. Conclusion

We have fabricated the nano-aperture array with nanoscale double slits, in addition to the nanoscale double slits. For nanoscale double slits, we observed the highest optical intensity at slits separations of 5 μm, and higher intensities at the 15 μm slit-pitch than others due to surface plasmonic interference. For nano-aperture (7 × 7) array with a 530 nm aperture-pitch sidelined with the nanoscale double slits, the highest enhancement factor of ~8.4 at 719 nm peak position is obtained. However, the significant reduction of the transmitted optical intensity is observed from the nano-aperture array surrounded with 4 nano-slits. The nanoscale aperture platform with huge optical enhancements can be utilized as a next generation bio sensor device.

CRediT authorship contribution statement

Seong Soo Choi: Conceptualization, Data curation, Formal analysis, Funding acquisition, Investigation, Methodology, Writing - original draft. **Sae-Joong Oh:** Funding acquisition, Investigation, Methodology, Writing - review & editing. **Yong Min Lee:** Funding acquisition, Investigation, Methodology, Writing - review & editing. **Hyun Tae Kim:** . **Soo Bong Choi:** . **Byung Seong Bae:** Writing - review & editing.

Declaration of Competing Interest

The authors declare that they have no known competing financial interests or personal relationships that could have appeared to influence the work reported in this paper.

Acknowledgements

This work was supported by the research funding programs (Development of Biofriendly Optical Nanopore, 2018R1D1 A1B07050106) under the Basic Science Research Program, and by Nano-Material Technology Development Program (funding No: 2018M3A7B4069997) through the National Research Foundation of Korea (NRF), funded by the Ministry of Education, Science and Technology, South Korea, and also funded by Ministry of Science and Information & Communication Technology.

References

[1] M. Muthukumar, C. Plesa, C. Dekker, Phys. Today 68 (2015) 40–46.
[2] A. Mikheyev, M.M.Y. Tin, Mol. Ecol. Resour. 14 (2014) 1097–1102.
[3] E.C. Hayden, Nature 521 (2015) 15–16.
[4] T.W. Ebbesen, H.J. Lezec, H.F. Ghaemi, T. Thio, P.A. Wolff, Nature 391 (1998) 667–669.
[5] H.J. Lezec, A. Degiron, E. Devaux, R.A. Linke, L. Martin-Moreno, F.J. Garcia-Vidal, T.W. Ebbesen, Science 297 (2002) 820–822.
[6] D.W. Kim, Y.C. Kim, O. Suwal, V. Jha, M.J. Park, S.S. Choi, Mater. Sci. Eng. B 149 (2008) 242–246.
[7] S.S. Choi, O.K. Suwal, V. Jha, D.W. Kim, M.J. Park, Curr. Appl. Phys. 9 (2009) S131–S133.
[8] S.S. Choi, M.J. Park, C.H. Han, Y.S. Kim, N.K. Park, S.H. Han, H. Choo, J. Vac. Sci. Technol. B 33 (2015) 06F203.
[9] A. Nahata, R.A. Linke, T. Ishi, K. Ohashi, Opt. Lett. 28 (423) (2003) 423–425.
[10] Y. Liu, S. Blair, Opt. Lett. 28 (2003) 507–509.
[11] E. Altewischer, M.P. van Exter, J.P. Woerdman, Nature 418 (2002) 304–306.
[12] R. Gordon, A.G. Brolo, A. McKinnon, A. Rajora, B. Leathem, K.L. Kavanagh, Phys. Rev. Lett. 92 (2004) 037401.
[13] S.S. Choi, S.J. Oh, C.H. Han, N.K. Park, Y.S. Kim, J.H. Yoo, K.J. Park, Surf. Coating. Technol. 306 (2016) 113–116.
[14] S.S. Choi, M.J. Park, T. Yamaguchi, C.H. Han, S.J. Oh, S.I. Kim, K.J. Park, J.H. Yoo, Y. S. Kim, N.K. Park, Sens. Bio-Sens. Res. 7 (2016) 153–161.
[15] S.S. Choi, M.J. Park, T. Yamaguchi, S.I. Kim, K.J. Park, N.K. Park, Appl. Surf. Sci. 310 (2014) 196–203.
[16] S.S. Choi, S.J. Oh, C.H. Han, D.J. Park, S.B. Choi, Y.S. Kim, N.K. Park, J. Vac. Sci. Technol. B. 35 (2017) 04F107.
[17] H.F. Schouten, N. Kuzmin, G. Dubois, T.D. Visser, G. Gbur, P.F.A. Alkemade, H. Blok, G.W'.t. Hooft, D. Lenstra, E.R. Eliel, Phys. Rev. Lett. 94 (2005) 053901.
[18] C.H. Gan, G. Gbur, T.D. Visser, Phys. Rev. Lett. 98 (2007) 043908.
[19] M. Verma, S. Joshi, N.S. Bisht, H.C. Kandpal, P. Senthilkumaran, J. Joseph, J. Opt. Soc. Am. 29 (2012) 195–199.

Please cite this article as: S. S. Choi, S. J. Oh, Y. M. Lee et al., Towards the ultrafast optical nanopore platform for single molecule sensing, Materials Today: Proceedings, https://doi.org/10.1016/j.matpr.2020.01.359